Advances in Environmental Technology 4 (2022) 255-270

Iranian Reasearch Organization for Science and Technology (IROST)

Advances in Environmental Technology

Journal home page: https://aet.irost.ir/

Optimization of an activated sludge process equipped with a diffused aeration system: Investigating the diffuser density sensitivity

El Aissaoui El Meliani Mohamed El Amine [a*], Sun Meng [b], Amen Tareq W. M.[c], Choubane Houcine [d], Iddou Abdelkader [a], Liu Bing [e], Terashima Mitsuharu [b]

[a]*Saharan Natural Resources Laboratory, Faculty of Science and Technology, Ahmed Draia University, Algeria*

[b]*Recycle Engineering Laboratory, Faculty of Environmental Engineering, The University of Kitakyushu, Japan*

[c]*Laboratory of Inorganic Materials and Soft Chemistry, Department of Life, Environment and Applied Chemistry, Graduate School of Engineering, Fukuoka Institute of Technology, Japan*

[d]*Laboratory of Organic Synthesis, Physico-chemistry, Biomolecules and Environment, Department of Chemical Engineering, University of Science and Technology of Oran Mohamed Boudiaf, Algeria*

[e]*Resources and Environment Innovation Research Institute, School of Municipal and Environmental Engineering, Shandong Jianzhu University, China*

ARTICLE INFO

Document Type:
Research Paper

Article history:
Received 5 February 2022
Received in revised form 29 October 2022
Accepted 1 November 2022

Keywords:
Power consumption
Pressurization effect
Aeration efficiency
Taguchi-Grey method
Activated sludge
Local diffuser density

ABSTRACT

The present work investigates the aeration pressurization effect by monitoring the airflow (Q_g) variations during its injection at various diffuser arrangements in an activated sludge (AS) system and its impact on the overall energy-saving strategy. To this extent, a laboratory pilot-scale system (450 mm in length, 400 mm in width, and 470 mm high) was built to conduct the experiments with an effective volume of 84.6 L. To determine the optimum operating conditions, an experimental design combined with the grey method was used to establish the optimal tests to minimize the process's energy footprint based on the pressurization effect due to various diffuser arrangements. Successful implementation of this operation confirmed that controlling the local diffuser densities (DD_L) benefits the power consumption value by experiment (P_{Ef}) savings and the mixing performances at a DD_L = 0.0144. Undoubtedly, increasing the DD_L improved the mixing performance of the AS and reduced the inhibition of the oxygen mass transfer coefficient by the mixed liquor suspended solids (MLSS). Furthermore, an empirical model was built to describe the nature of the power consumed accurately. The outcomes showed that the coefficient of determination was R^2 = 0.9856 with a significant corresponding probability (P-values) < 0.05. As a result, the multiple linear regression model (MLR), which means that the model's reliability to predict the

*Corresponding author: Tel: +(213) 555-647-722
Email: mohamedelamine.elaissaouielmeliani@univ-usto.dz
DOI:10.22104/AET.2022.545.1479

data revealed an R^2 > 80 %, confirmed that the model is reliable at a 95% confidence interval (CI).

1. Introduction

The activated sludge (AS) process is a WRRT that uses a biological process for treating municipal or industrial wastewater using aeration and biological flocs composed of bacteria and protozoa [1]. It is considered an intensive energy consumption process with a significant margin for improvement [2]. Therefore, throughout the development of the AS configurations, it appears that the need for oxygen to support aerobic biokinetics has included the operation of aeration systems as an integral part of water resource recovery [3]. According to Wang [4], supplying air to biomass requires the highest energy use, accounting for more than 50 % of the net power demand, representing a significant fraction of total costs, ranging from 50 % to 80 %. It has been estimated that the energy used in wastewater treatment plants (WWTPs) comprises around 1/5 of a municipality's total energy use by public utilities, and it's supposed to rise to more than 20 % in the next 15 years with increasing water consumption and more strict regulations [5]. In most of the medium and the large WWTPs with conventional AS systems, aeration takes up approximately 50–60 % of all electricity consumption [6], while sludge treatment consumes 15-25 % of energy, followed by secondary sedimentation, including recirculation pumps (15 %) [7,8]. Uniform arrangement (air flow rate, the depth of submergence of the diffusers, and the diffuser density) is considered the main essential factor in the aeration system [9]. The influence of the airflow rate, depth of submergence, and diffuser density on the specific oxygen transfer efficiency (SOTE) and specific oxygen absorption (SOA) are well documented in the literature by Wagner et al. [10]. Oxygen deficiency may significantly affect the process performance since the chemical and biological processes have low aqueous solubility and high demand [11]. Modern, well-designed, and operated aeration systems can achieve SOTE values between 8.5 and 9.8 %. m^{-1} [12]. Garrido et al. [13] showed that during the first year of operation, the initial energy use of aeration diffusers located in high-rate systems increased by more than 20% compared to the conventional methods. Diffusers operating for three years in traditional techniques presented the same fouling characteristics as those deployed in high-rate processes for less than 15 months. The energy consumption of the aeration system depends both on the blower's efficiency and the characteristics of the influent wastewater load [14], which require more attention and control. For this purpose, several investigations have been considered over the last few years. Nguyen et al. [15]worked on optimizing aeration time using the activated sludge model (ASM1) and benchmark simulation model (BSM1) for energy saving. Many approaches were compared regarding energy and the carbon footprint [16]. In investigating high airflow rates per diffuser, it was used to prevent diffuser biofouling and keep biological solids in suspension [2,17]. It was also used to quantify the oxygen transfer and uptake in integrated fixed-film activated sludge (IFAS) systems [18]and to study the variation of aeration diffuser efficiency over time while concurrently analyzing the energy consumption variations for each diffuser [13]. Another alternative was based on the design of experiments, which has primarily proven its reliability in studies related to wastewater treatment. It was used to determine significant process parameters that influence the hydrodynamics of the volumetric oxygen mass transfer coefficient K_La, as studied by Gori et al. [14] and Terashima et al. [19]. The possible behaviors of the airflow (Q_g), air passage section (S_a), and wastewater volume (V_L) on the (α)-factor prediction are determined using an experimental design, which leads to a reduction of the total number of experiments performed [20]. Therefore, it is easy to emphasize the aeration's energy demand from the available literature. According to Nazari et al. [21], reducing the number of experiments could affect power saving, the chemical oxygen demand (COD) removal, and the microbial community. Indeed, it is clear that the hydrodynamic parameters associated with the control and geometry of the aeration basin and the sludge concentration affect the amount of air injected into the aeration basin, leading to higher or lower consumption of energy according to the situation. During the execution of some of this work's experimental tests, it was noticed that at low aeration conditions (minimum Q_g values), the pressure force exerted by the wastewater was greater than the pressure force of the injected air, implying poor performances for both aeration and mixing. Indeed, this explains the difficulties encountered by the injected air to generate enough bubbles at diffuser orifices. To remedy this problem, a re-organization of the diffuser arrangements used in this investigation was considered. Moreover, as pressure is defined as being a force applied on a surface, it was judiciously assumed that reducing the number of active diffusers limits the surface on which the pressure of the injecting air exerts a force. This approach, called "pressurization", should make it possible to enhance air bubble generation and provide an ideal mixing of the activated sludge, allowing good contact between the microorganisms and the injected air bubbles. By considering what was mentioned above, it can be stated that the aeration systems have not been the central focus when investigating the pressurization effect and its significant margin of improvements in power savings. This work focused on the impact of the injected air's pressure fluctuations at various diffuser arrangements in the AS process to enhance the aeration and improve the contact between air bubbles and the mixed liquor suspended solids (MLSS) for a better overall energy-saving strategy. An experimental design was used to minimize the number of experiments in the process and focus on operational factors such as the (Q_g), the diffuser depth (d_i), the local diffuser density (DD_L), and on the performances of the AS aeration. Additionally, an empirical model that describes the nature of the power consumed for an accurate evaluation of the overall energy-saving strategy was also aimed. Engineers can subsequently use this model to evaluate the aeration tank's power consumption for cleaner treatments and uses once implemented in the WWTPs.

2. Material and methods

2.1. Experimental analysis

2.1.1. Configuration of the experimental set-up and testing procedures

The lab-scale pilot (aeration basin) used in this study was fabricated from glass, and it had a sufficient volume of 84.6 L, a length of 450 mm, a width of 400 mm, and a height of 470 mm. The aeration basin was equipped with six diffusers of 1 mm diameter of the orifice hole, connected to a glass rotameter that regulated the airflow ranging between $1000 < Q_g < 4000$ L-Air h^{-1}. The air was supplied through an ARENES air compressor equipped with a YL801-2 series single-phase motor (72 % motor efficiency) with a flow rate of 200 L/min. The tap water and AS temperature were maintained at 27 °C using a thermostat. Two sets of these devices were used in this experiment, as shown in Figure 1. In this aeration basin, tap water under discontinuous aeration conditions (no influent or effluent water flow) was investigated (Figure 1. (B)). To remove the dissolved oxygen (DO) from the water, Na_2SO_3 was added in the presence of the cobalt catalyst $CoCl_2$. The sulfite concentration was sufficiently low not to alter the properties of the water, knowing that to decrease the DO by 1 mg O_2. L^{-1}, 7.9 mgL^{-1} Na_2SO_3 was needed [23]. After reaching a DO concentration of 0 mg O_2. L^{-1} in the basin, the aeration was turned on. The air was injected upward through the diffuser. The concentration of DO and the water temperature were measured in the basin using a waterproof oximeter, Hanna Instrument HI 98193 (± 0.5%), with a time step of 10 seconds of acquisition between each point.

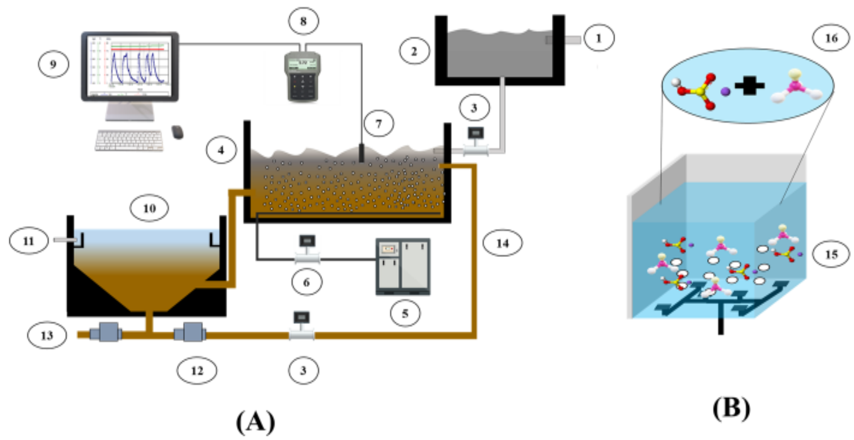

1	Influent Wastewater	5	Air Compressor	9	Computer with Data Acquisition	13	WAS
2	Synthetic Wastewater Bassin	6	Rotameter	10	Settling Tank	14	RAS
3	Liquid Flowmeter	7	DO Probe	11	Effluent Water	15	Tap Water Basin
4	Aeration Basin	8	Oximeter	12	Hydraulic Pupm	16	$Na_2SO_3 + CoCl_2$

Fig. 1. Experimental lab-scale pilot representation: (A) activated sludge, (B) tap water.

Regarding the wastewater tests, the aeration basin contained AS with excellent settleability quality, operated at 27 °C, as shown in Figure 1. (A). The AS used in the tests was collected from (Cap-Falcon-WWTPs, Oran, Algeria) within 24 h after sampling with a sludge retention time (SRT) of 19 days. The pH was maintained at around 7.0 at the beginning of each cycle by adding sodium hydroxide solution (0.2 M). The composition of the AS in terms of carbon, nitrogen, and phosphorous compounds was measured in the WWTPs laboratory as listed in Table A1 (data appendix). Synthetic wastewater (SWW) was then added to the AS present in the aeration basin with an influent flow rate of 1.4 L/min to maintain the biological cycle by feeding the microorganisms present in the AS. The air was injected upward through the diffuser. The concentration of DO and the water temperature were measured in the basin using a waterproof oximeter, Hanna Instrument HI 98193 (± 0.5%), with a time step of 10 seconds of acquisition between each point. The SWW was prepared according to the standard method shown in [22], and it was composed of (16 g/L of peptone; 3 g/L of urea; 0.7 g/L of NaCl; 0.4 g/L of $CaCl_2$; 0.2 g/L of $MgSO_4$ and 2.8 g/L of K_2HPO_4). To maintain similar concentrations for all the tests, $\pm$2.5 g/L of the sludge was diluted with filtered wastewater effluent and then added to the SWW. Afterward, the wastewater flowed from the aeration basin to a cylindrical settling basin. A part of the sludge was recycled to the aeration basin (15 % of the total sludge flow) using a hydraulic pump (Taifu-GRS12/9-Z). The whole experimental period was divided into four operational phases according to the influent airflow rate: Phase I (4 days), Phase II (4 days), Phase III (4 days), and Phase IV (4 days). After each phase, a diffuser was added to the reactor, and a liquid level controller controlled the height of the AS in the aeration basin to estimate the load due to air distribution (ΔH).

2.1.2. Oxygen transfer coefficient Prediction

Each basin's water volumetric mass transfer coefficients (K_La) were determined using the ASCE methodology [24]. The total change in concentration over time due to aeration is described by Equation (1), considering the liquid phase in equilibrium with the gas phase and that of K_La, which is typically used in WWTPs modeling to quantify the aeration [25]. The rate change of the DO was then calculated, which is indicative of the OTR reduced by the OUR [29,30]. Care was taken to obtain adequate sampling during the initial ascension portion of the DO-time curve and to allow the system to reach a quasi-steady-state condition at the end of the test.

$$\frac{dC}{dt} = OTR - OUR = K_La(C_S - C) - OUR \quad (1)$$

Equation (2) can be integrated from the time, t_1, at which the airflow started to any subsequent time, t_2, to give:

$$K_L a = \frac{\ln[(C_S - C_1)/(C_S - C_2)]}{t_2 - t_1} \quad (2)$$

For the prediction of the oxygen saturation concentration (C_S), a temperature-dependent (T) equation could be used [23]:

$$C_S = 14.652 - (0.41022 \times T) + (7.9910 \cdot 10^{-3} \times T^2) - (7.7774 \cdot 10^{-5} \times T^3) \quad (3)$$

t_1 and t_2 are usually chosen as the measured oxygen concentration that is 20% (t_1) and 80% (t_2) of the saturation values for the tested water, corrected for temperature and barometric pressure. This study used 20 and 75% saturation values for t_1 and t_2 since many data points were collected between these values. The measurement of OUR in situ would be an excellent indicator for the prediction of K_La_f, where the DO, OUR, q_{O_2}, and temperature were measured with a waterproof oximeter (HI 98193). Once the OUR and q_{O_2} values were available, it was easy to obtain the evolution of the biomass using the following equation:

$$OUR = q_{O_2} \times X_B \quad (4)$$

2.1.3. Diffuser density

The diffuser density (DD) is described as the ratio of the total surface of the perforated membranes or diffuser to the tank area. However, Gillot et al. [9] introduced the term local diffuser density (DD_L), which is the ratio of the total surface of the perforated membranes to the aerated area. Similar to the concept of Gillot et al. [9], the DD_L of a rectangular diffuser (Figure 2) is assumed in this investigation as follows:

$$DD_L = (S_{OR} \cdot N_{OR}/S_{dif}) \cdot N_{dif} \quad (5)$$

2.1.4. The experimental power consumption measurement

The measurement of the power consumed in the case of aeration by air diffusion is generally used as a significant indicator of the technical-economic studies to choose which type of installation offers low costs. However, this can be expressed, thanks to the airflow and the load due to air distribution, as demonstrated [26]:

$$P_E = \frac{Q_g \cdot \rho \cdot g \cdot (d_i + \Delta H)}{\eta} \quad (6)$$

The most common parameter describing energy efficiency is the aeration efficiency (AE, $KgO_2.kW^{-1}.h^{-1}$), defined as:

$$AE_f = \frac{SOTR_f}{P} \quad (7)$$

2.2. Statistical Analysis

2.2.1. Taguchi's approach

This experimental design method is generally preferred because it dramatically reduces the number of experiments [27]. For this investigation, three parameters (the airflow, the diffuser depth, and the diffuser density) were selected as those likely to have the most significant influence on the power consumed (PE_f), as listed in Table 1. However, the operational levels of Table 1 have been selected based on the geometric configuration of the aeration basin in terms of volume and surface and based on the range of the airflow variations proposed by the glass rotameter, which was used in this investigation.

To design the Taguchi plan and its subsequent analysis, the (Minitab Statistical Software, Pennsylvania, USA) was used to provide a set of experiments performed according to a determined order. The program was based on the of orthogonal matrices that help to plan a set of experiments that the experimenter desires to achieve. An appropriate orthogonal array (OA) L_{16} (4^{3-1} = 16) was selected to perform this research experiment, as listed in Table 2.

Table. 1. Controlling factors and their levels.

Factors	Units	Symbols	Level-1 +	Level-2 ++	Level-3 +++	Level-4 ++++
X_1: Airflow	cm^3/s	Q_g	126.12	252.22	378.33	504.44
X_2: Diffuser density	[-]	DD_L	0.0087	0.0115	0.0144	0.0173
X_3: Diffuser depth	cm	d_i	21.000	26.000	31.000	36.000

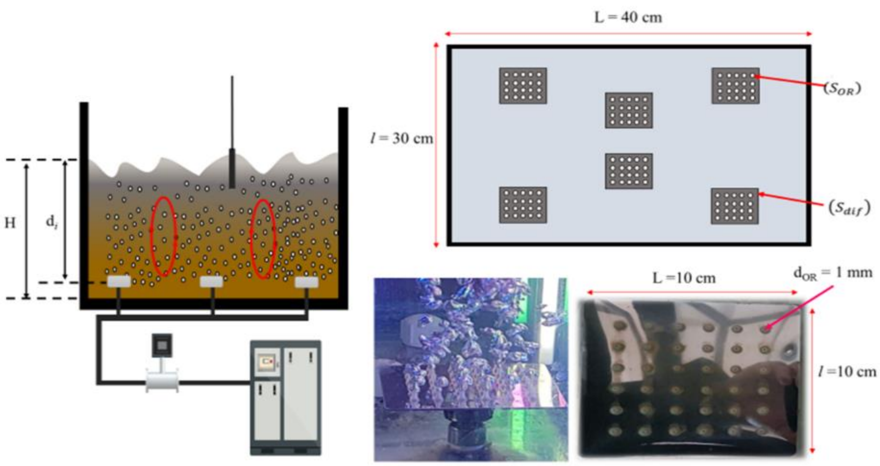

Fig. 2. Relevant DD_L characteristics in the aeration tank.

Table 2. Taguchi orthogonal matrices (OA) - L_{16}.

Days	Coded values			Factor Values				
	X_1	X_2	X_3	Q_g [cm^3/s]	DD_L [-]	d_i [cm]	Q_g [Kg/s]	d_i [m]
1	+	+	+	126.12	0.8481	45	0.00073	0.45
2	+	++	++	126.12	1.1308	54	0.00073	0.54
3	+	+++	+++	126.12	1.4135	63	0.00073	0.63
4	+	++++	++++	126.12	1.6962	72	0.00073	0.72
5	++	+	++	252.22	0.8481	54	0.00150	0.54
6	++	++	+	252.22	1.1308	45	0.00150	0.45
7	++	+++	++++	252.22	1.4135	72	0.00150	0.72
8	++	++++	+++	252.22	1.6962	63	0.00150	0.63
9	+++	+	+++	378.33	0.8481	63	0.00220	0.63
10	+++	++	++++	378.33	1.1308	72	0.00220	0.72
11	+++	+++	+	378.33	1.4135	45	0.00220	0.45
12	+++	++++	++	378.33	1.6962	54	0.00220	0.54
13	++++	+	++++	504.44	0.8481	72	0.00290	0.72
14	++++	++	+++	504.44	1.1308	63	0.00290	0.63
15	++++	+++	++	504.44	1.4135	54	0.00290	0.54
16	++++	++++	+	504.44	1.6962	45	0.00290	0.45

2.2.2. Analysis of variance (ANOVA)

In this study, an ANOVA test was performed using Minitab Statistical Software (Pennsylvania, USA) to determine which factors were significant and had a positive or negative effect on the specified responses. Performing the ANOVA analysis led to correlating the target responses based on the input variables mentioned in the OA. The general form of the equations is expressed as:

$$Y = a + b_1X_1 + b_2X_2 + b_3X_3 \tag{8}$$

where Y represents the response function of the regression model and a, b_1, b_2 and b_3 are the partial regression coefficients for the variables X_1, X_2, and X_3, respectively. For measuring devices under field conditions, statistical tests were conducted to validate the preconditions of linear regression. Sarıkaya et al. [28] also recommended evaluating an experimental design at a 95% confidence level. The confidence interval calculation was based on the measured data to control the error within a suitable range [29]. The following Equation calculated the confidence interval:

$$\bar{x} - SD\sqrt{\frac{F^{1}_{n-1}(a)}{n}} \leq \mu \leq \bar{x} + SD\sqrt{\frac{F^{1}_{n-1}(a)}{n}} \quad (9)$$

Where the standard deviation is calculated as follows

$$SD = \sqrt{\frac{\sum(x_i - \bar{x})^2}{n-1}} \quad (10)$$

*2.2.3. Grey relationship analysis (**GRA**)*

The grey relational analysis (GRA) method converts an optimization problem with several performance characteristics into a single objective optimization problem. To perform this analysis, some steps are necessary [30]. First, the normalization converts the original values found in Table 2, ranging between 0 and 1 [31]. Normalization was implemented according to the type of performance characteristics required and can be calculated using the following relationship:

$$x^{*}{}_{i}(k) = \frac{x_i(k) - x_i(k)}{x_i(k) - x_i(k)} \quad (11)$$

After the normalization process, the next step is to calculate the grey relational coefficient (GRC) from the normalized values obtained using the following formula:

$$GRC = \frac{\Delta_{min} + \varphi\Delta_{max}}{\Delta_{0i}(k) + \varphi\Delta_{max}} \quad (12)$$

$$\Delta_{0i} = \|x_0(k) - x_i(k)\| \quad (13)$$

The grey relational grade (GRG) is then determined by averaging the grey relational coefficients corresponding to each performance characteristic and can be expressed as follows:

$$GRG = \frac{1}{n}\sum_{k=1}^{n} \xi_i(k) \quad (14)$$

A response table can display the average grade values for each process parameter grade. The highest-grade values are chosen as the optimal parametric combination for the multiple responses.

3. Results and discussion

Numerous experimental results are reported in this section for both clean water and AS systems, where the management of an overall energy-saving strategy was maintained as the ultimate goal. The first operational step of this investigation was to monitor the DO for both tap water and AS to observe how it behaved and use its data to evaluate the accuracy of the oxygen mass transfer in both fluids mentioned above. Next, the observed sensitivities that the oxygen mass transfer showed due to the effect of DD_L, the MLSS and the biomass variations were discussed to reveal their impact on the aeration efficiency's adopted actions to reduce power consumption. Moreover, statistical calculations were employed to build a new empirical model for the power consumed prediction explanation. Once these experimental findings were explained, an optimization was performed using the Grey method to reveal the best parameters combination for an efficient process operation with low energy usage.

3.1. Dissolved oxygen monitoring

During the tests carried out in the laboratory, it was observed that the concentration of oxygen increased with the injected airflow; therefore, it became clear that the airflow controlling the injection process through the orifices affected the time necessary for the dissolved oxygen to reach saturation, see Figure 3 (a). Indeed, a passage from the stable regime of 1000 L/h to a turbulent regime between 1500 and 3000 L/h supported the observations made in the laboratory where the aeration time goes from 1840 s for a flow rate from 430 L/h to 80 s at 4000 L/h to reach a concentration of 10 mg/L at which it saturates with an average SD of ± 0.5 mg O_2. L^{-1}. Next, the aeration was carried out in a bioreactor operating at oxygen saturation concentration intervals between 75% C_s as the maximum value and 20% C_s as the minimum value. The results obtained were precise and corresponded to the operating data obtained at the WWTP from where the AS were taken. It is noted that the variation range was between 5.5 and 7.2 mg O_2. L^{-1} with an average SD of ± 0.44 mg O_2. L^{-1} (Figure 3 (b)).

3.2. Oxygen mass transfer coefficient

Clean water oxygen transfer testing was performed to assess the K_La at different stages of the aeration operations occurring in the clean water. At a fixed aeration flow rate (AFR) ranging between 126.12 - 252.22 cm^3/s, the estimated K_La was up to 0.0095 - 0.0207 s^{-1} (34.2 - 74.52 h^{-1}), which was higher than the ones reported by Painmanakul et al. [32]. However, the reported K_La varied more intense at higher AFR around 252.22 - 504.44 cm^3/s, where the overall variations were reported between 0.0207 – 0.1022 s^{-1} (74.52 – 367.92 h^{-1}) with an average SD of ± 0.09 s^{-1} (Figure 4). The range and the values reported in this study were high, which make the comparison with the reported results of Sodeifian et al. [33], Gillot et al. [34], Fan et al. [35], and Trambouze et al. [36]challenging to realize. This might be explained because the performed experiments were executed in a more extensive geometry system using only one DO sensor [32]. According to Baquero et al. [3], for bubble column aeration systems with a liquid volume of 0.01 to 3000 m^3, the K_La range required for the correct functioning of the basin should be around 0.01 – 0.2 s^{-1}. These results agree with the trends recorded by Al-Ahmady et al. [37], who reported a K_La range of 2.2 – 106 L/h for a rectangular batch reactor. In this case, agreements were mainly due to similarities in geometrical and hydrodynamical parameters. Regarding the AS, the dynamic K_La_f tests were performed under various mixing and volumetric airflow rate conditions using WWTPs mixed liquor to facilitate direct comparisons between the two cases (tap water and wastewater). The resulting K_La_f values determined in AS experimentations showed that the the K_La_f of days one to four decreased from 0.0041 s^{-1} to 0.0018 (14.76 h^{-1} to 6.48 h^{-1}) in Figure 4. Then, from day four to day 10, an elevation of the oxygen transfer was noticed, ranging between 0.0018 – 0.0114 s^{-1} (6.48 – 41.04 h^{-1}) with an average SD of ± 0.006 s^{-1}. The reported results of K_La_f observed from day 11 until day 16 showed unstable fluctuations, where K_La_f decreased to a low value on day 12 equal to 0.0065 s^{-1} (23.4 h^{-1}) before it started rising again on day 13 and reached a value of 0.0295 s^{-1} (106.2 h^{-1}). Finally, it was observed that the K_La_f decreased again on day 14 and kept a stable range reported between 0.0093 – 0.0114 s^{-1} (33.48 – 41.04 h^{-1}) until day 16. These results indicated that oxygen transfer performances were affected by the MLSS variations, as shown in Figure SM.1 (supplementary material). The MLSS increase led to an exponential decrease of K_La_f as it hinders oxygen fluxes due to microorganisms absorbing the air bubble [38]. According to Lee [39], the solid particles composing the MLSS flocs increased the bulk liquid's apparent viscosity and blocked the interfacial bubble area, reducing mass transfer. The findings showed that an increasing influent COD concentration reduced the K_La_f.

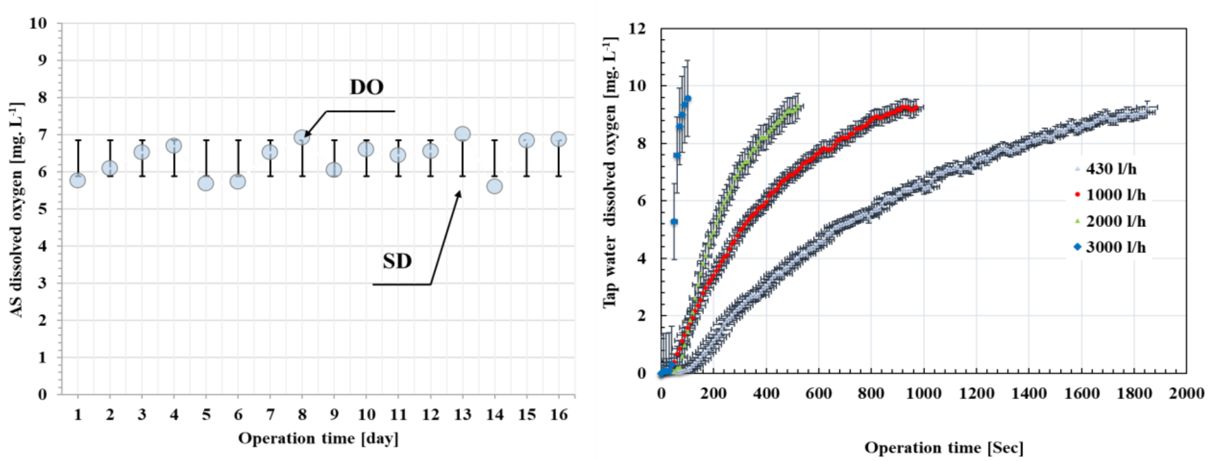

(b) Activated sludge's DO profile **(a) Tap water's DO profile**

Fig. 3. Dissolved oxygen scatter plot for (a) Tap water and (b) AS.

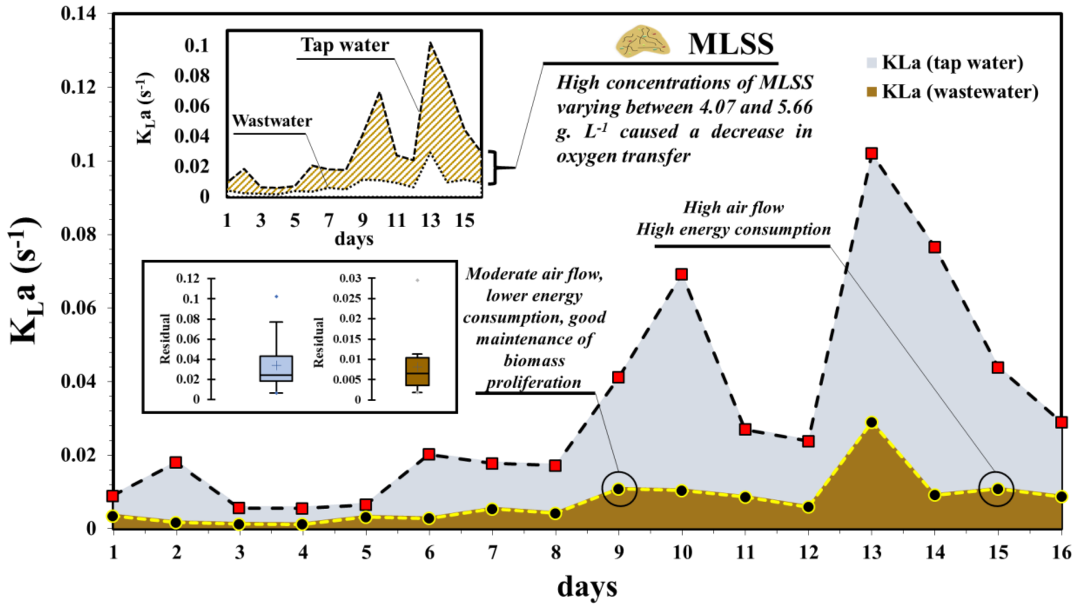

Fig. 4. Experimental observations of K_La in both tap water and AS tests.

3.3. Diffuser density impact

The operational influence of the DD_L on the aeration efficiency is summarized in Fig. 5. The phase I results obtained for tap water aeration revealed some unstable variations of K_La. The causes of these variations can be explained by an insufficient or excessive implementation of the diffusers in the aeration basin. Typically, an increase in diffuser density is expected to result in a higher OTE [17]. According to Uby [40], increasing the number of diffusers from 1 to 2 at a constant airflow rate produced a 25% increase in K_La. In phase II and phase III, the chosen diffuser arrangements showed excellent performance in terms of oxygen transfer than phase I. The increases in aeration rates resulted in an increasing OTR, potentially because of the effects of turbulence caused by aeration, as shown in Figure SM.1. Moreover, the addition of diffusers operated at a moderate AFR resulted in the formation of an ellipsoidal bubble. For phase IV, the reported results clearly show that K_La decreased when the DD_L was increased at its highest value, combined with a high ARF. For AS, the results diverged for all the phases because the K_La_f decreased due to insufficient mixing. Typically, the test standard situation with oxygen consumption and the increased effective viscosity, as mentioned by Skouteris et al. [41], was essential in the mixing operation for the BOD, nutrient removal, and sludge characteristics. Exceptions were observed in phases II, III, and IV when the DD was equal to 0.0144, and the DO distribution was performing excellent mixing hydrodynamics with moderate AFR requirements. This could be due to the different arrangement of the diffusers in the basin, which varies the pressurization and accelerate the oxygen transfer rates (OTR_f) by increasing the partial pressure of air [10].

3.4. Mixed liquor and biomass behaviors

The resulting values of OUR and q_{O_2} measured in situ by monitoring the concentration of DO during and after aeration showed sensitive interactions between DO, OUR, q_{O_2} and X_B (Figure 6). In the first stage, OUR goes through the exponential growth phase where high rates of DO consumption were observed. During the second stage, OUR decreased due to a decrease in the metabolic activity of cells in the absence of mixing. It is consistent with the studies of [43], where OUR varied from 6 to 11 mg. $L^{-1}.h^{-1}$, confirming the reliability of this research for OUR located between 5.51 to 16.24 mg. $L^{-1}.h^{-1}$ with an average SD of ± 0.5 mg. $L^{-1}.h^{-1}$. As oxygen consumption and biomass production rates decreased. Regarding the biomass, it is assumed that DO is one of its vital substrates, as illustrated in Figure 6. The observations show that the high value of q_{O_2}, which could be higher than OUR, decreased the development of the biomass X_B population thanks to the use of electron receptors under the operating conditions of the bioreactor. In this case, once the highest value of q_{O_2} became lower than OUR, the increases in the concentration of the X_B were noted between 4.1 and 5.8 mg/L with an average SD of ±0.53 g/L. These high biomass values explain the formation of solid aggregates in a wide DO concentrations range, ranging from 2 to 7 mg/L.

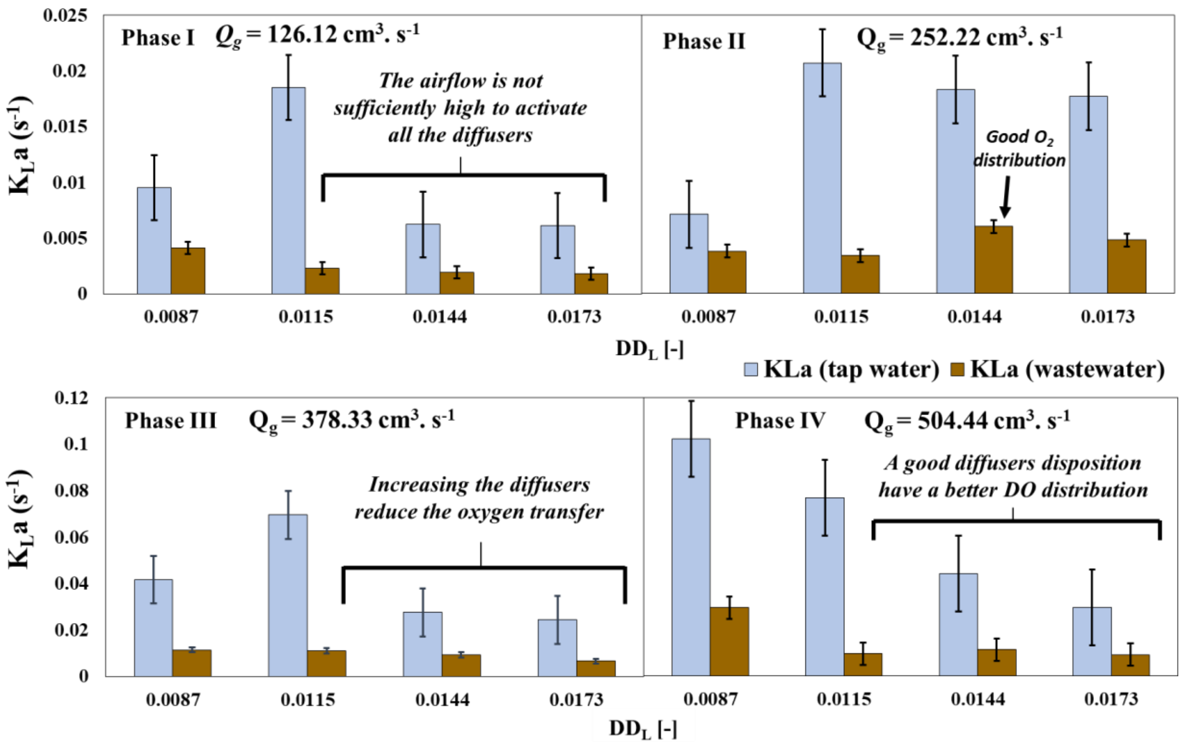

Fig. 5. The influence of the diffuser density on the oxygen transfer.

3.5. Aeration efficiency

Aeration systems should be purposely operated at less than optimum transfer efficiencies for reduced diffuser maintenance and improved mixing. In Figure SM.1 (supplementary material), it is observed that the SOTE of the aerobic reactor increases with the increasing load of air distribution because of the greater residence time of the bubbles and the more significant partial pressure of oxygen at the moment of bubble formation. As the partial pressure increases with diffuser depth, the operating pressure for the blower also increases [36]. The aeration efficiency characterizes the economy of an aeration system [10]. In Figure 7, the aeration efficiency is depicted as a function of the diffuser density. The results obtained are clustered according to different diffuser densities for tap water and wastewater. The reported AE ranges in both tap water and wastewater were respectively 0 – 0.0423 kgO_2. KW^{-1}. h^{-1} and 0 – 0.0119 $kgO_2.KW^{-1}.h^{-1}$ with an average SD of ± 0.0013 $kgO_2.KW^{-1}.h^{-1}$, showing that MLSS was not the only parameter that presents a strong sensitivity to understand the aeration control better. It must be noted that this study was limited to the BCB systems operating at high MLSS in which the positive effect of airflow rate gets altered. This finding is significant in understanding the true effects of MLSS on the AE_f and helping develop an effective strategy for process optimization and energy saving. However, all references point out that a comparison between different diffuser types is difficult because of the different calculations of the area of the orifices. This concern concerns modern, well-designed, operated aeration systems achievable with typical diffuser densities (15–35%) [16].

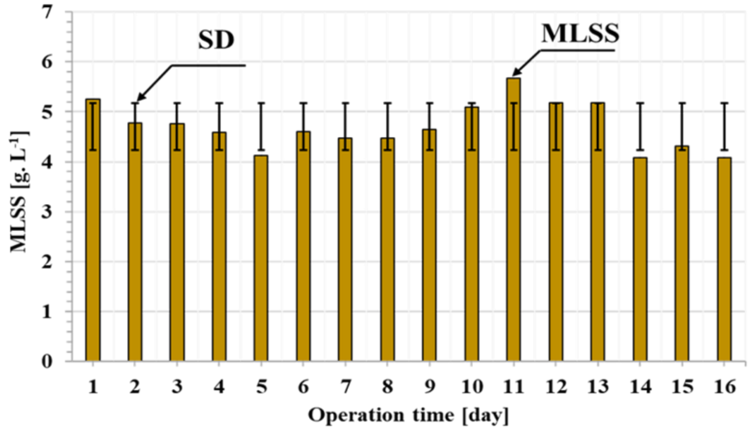

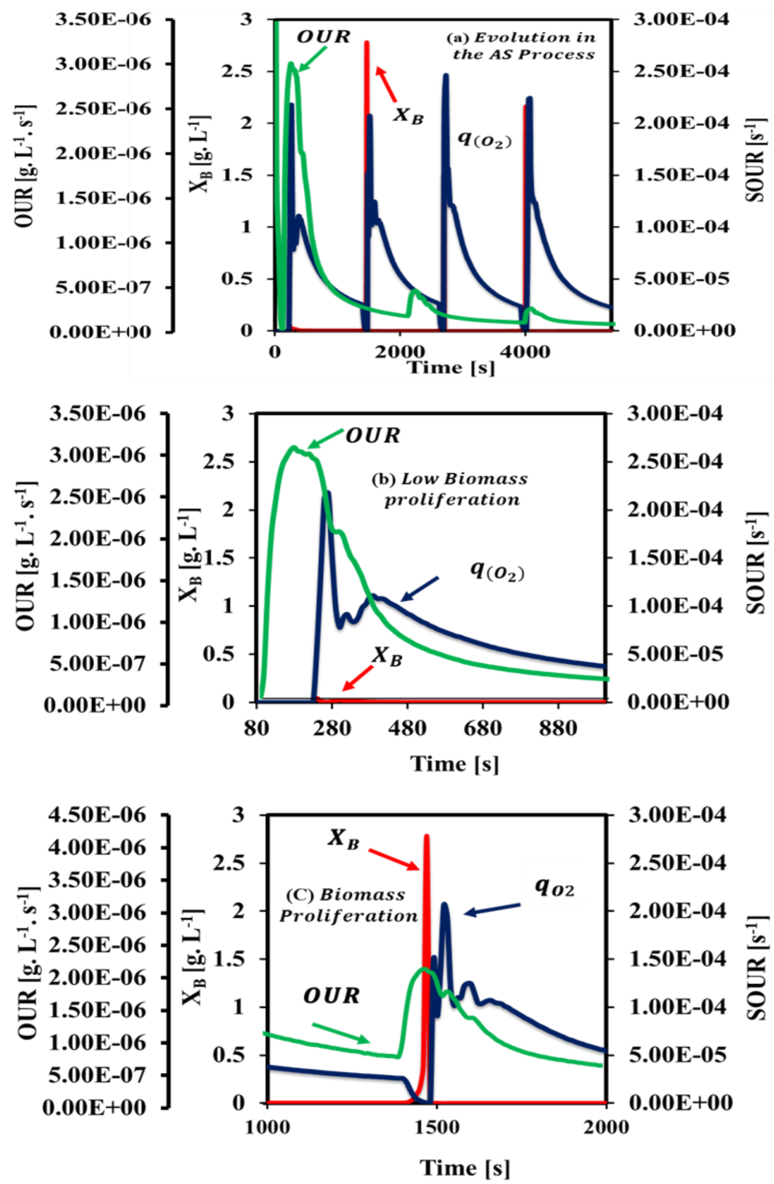

Fig. 6. Biomass evolution and respirometric parameters: (a) during the treatment, (b) biomass at the initial aeration stage, (c) biomass production during the treatment.

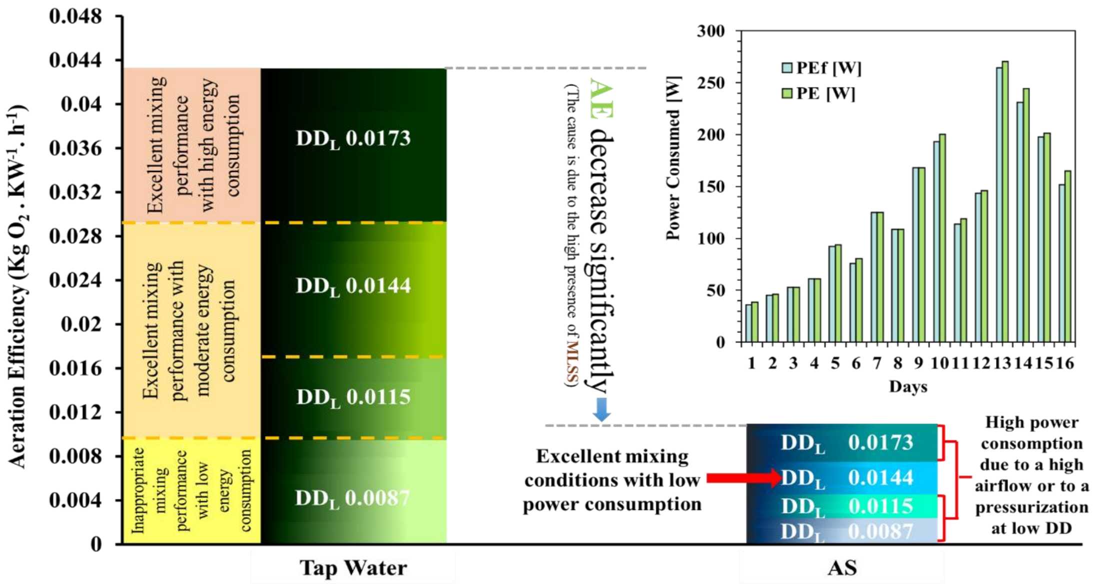

Fig. 7. Aeration efficiency and power variations as a function of the diffuser density.

3.6. *Power reduction and modeling*

Regarding the (P_E), the influence of the Q_g injected affects its rise due to a pressurization effect, making it vary from 36.29 W to 263.92 W for tap water with an average SD of ± 86 W, as shown in Figure 7. When MLSS are involved, an average decrease of 2.69 % in the previous range is observed. The variation of the number of diffusers in one single arrangement at various V_L and Q_g has also proved to be a valuable tool for optimizing (P_{Ef}) reduction and gives advantages such as excellent oxygen mass transfer, good biomass production, and moderate energy consumption. Then, using the experimental data, an empirical formula Eq. 15 was built to describe the sensitive nature of the Q_g, DD_L, and d_i for an accurate evaluation of the power consumption of the AS process. The results for the exponents and the coefficients' values based on the selected factors are given in Table 3.

$$P_{Pf}\ [W] = a + b_1 \cdot Q_g + b_2 \cdot DD_L + b_3 \cdot d_i \quad (15)$$

where Q_g is in (Kg/s), DD_L in (-), and d_i in (m). Additionally, an ANOVA test was performed to investigate the influence of the factors on the target variable. The corresponding probability (P-value) and the coefficient of determination R^2 are accurate indicators to verify the significance of factors interactions and realize an excellent prognosis. The results obtained from ANOVA show that the factors Q_g, DD_L, and d_i present the respective P-values: < 0.0001, 0.0013, and < 0.0001. The predicted R^2 was equal to 0.9868, and the adjusted-R^2 was equal to 0.9820. Since R^2 was equal to 0.9856 and knowing that the variables are insignificant when the P-values were higher than 0.05, it could then be assumed that the MLR could explain the power consumption variations. Fig. 8 shows the fitted scatter plots of the MLR model to explain the power consumption variations. The 95% confidence interval of the regression function was used to evaluate whether the deviation of the estimated linear regression model Eq.15 and the ideal relation was significant. The confidence interval must include the perfect association to guarantee no significant systematic error. The plot shows that the MLR model had a respective R^2 = 0.9856. The quality of the explanations presented an R^2 > 80 % which, according to Benmoussa et al. [42], confirmed that the model was reliable. Furthermore, the prediction interval in which the observations fall, with a certain probability, had given satisfying results for the MLR model.

Table 3. MLR exponents and ANOVA results.

Parameter estimates	Variable	Estimate	Standard error	95% CI (asymptotic)
a	Intercept	-112,7	17,25	-150,2 to -75,07
b_1	Q_g	-30,28	7,282	-46,15 to -14,42
b_2	DD_L	243,9	22,87	194,0 to 293,7
b_3	d_i	74922	2855	68702 to 81141

3.7. Grey's multi-objective optimization

The use of a multi-objective optimization method made it easy to combine the Taguchi OA and GRA to standardize the values of the responses for a better aeration performance. Figure 9 shows the importance of the GRC used to consider the GRG. It has been concluded that the highest GRG value gives an optimum characteristic response for the different tests. The arrangement of the experience N°.5 provided a high value of GRG and the most robust multi-performance combination of all 16 runs. These results confirmed that GRG identified the reference inputs' level of correlation and compared them to identify a clear interrelationship associated with a high GRG. Experience N°. 5 also had low P_{Ef} consumption rates due to a pressurization effect related to its diffuser arrangement and the long hold times of AS, which improved the operational performance and reduce the costs of the process. From what was mentioned above, it must be noted that this study was limited to BCB. The limits were mainly related to the geometric configuration of the lab-scale pilot, the controlled factors listed in (Table 1), and the daily variations of MLSS. However, the empirical model obtained showed strong reliability in describing (P_{Ef}). This model could be helpful to water treatment engineers who work on the conception of aeration tanks that aims to save power to reduce costs. The calculator could apply the formula to any diffused aeration case by adapting the coefficients and exponents to the data collected from the operating process using the excel solver tool.

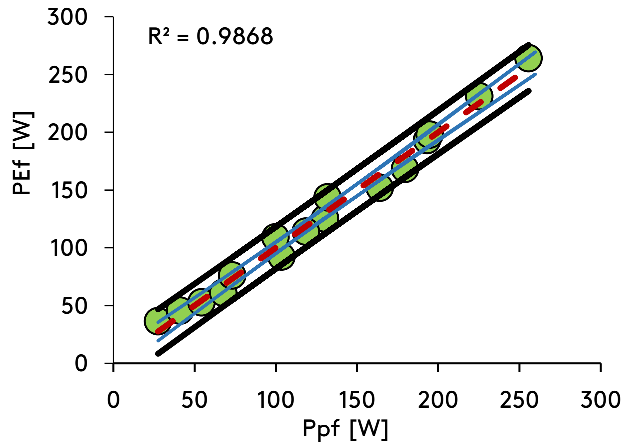

Fig. 8. Experimental Vs predicted values of the power consumed.

It could be concluded that controlling the DD_L has a clear benefit on the power consumption and the mixing performances of an AS process. A probable reason for this is that in the last 30 years, designers and manufacturers of aeration systems realized that this is a way to increase oxygen transfer. Therefore, the improvement may be due to a combination of improved diffuser efficiency and increased diffuser density with more efficient materials.

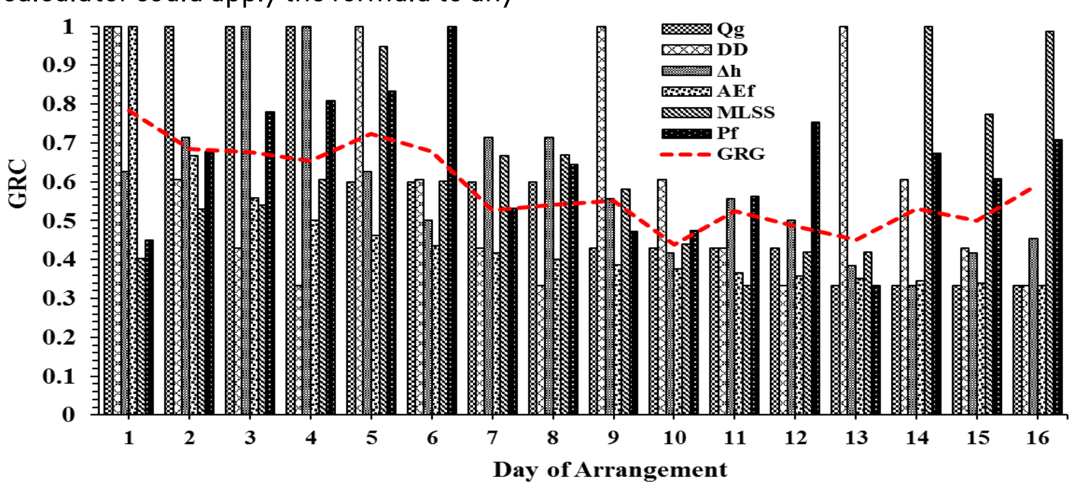

Fig. 9. Multi-objective optimization results.

4. Conclusions

To achieve an interdisciplinary goal in this work, we focused, in the first place, on the MLSS sensitivity effect on the aeration behaviors for better energy saving in the AS process. The following was then observed:

- The DO distribution was performing excellent mixing hydrodynamics with moderate AFR requirements. The reason was caused by the different number of diffusers in one single arrangement in the basin, which varied the pressurization and accelerated the OTR by increasing the partial pressure of air.

- The K_La_f decreased due to the MLSS increase. As reported from day one, the K_La_f decreased in the range reported between 0.0041 s^{-1} to 0.0018 (14.76 h^{-1} to 6.48 h^{-1}) until day four. These results indicated that oxygen transfer performance was mainly affected by the MLSS variations.
- The use of a multi-objective optimization method made it easy to combine the Taguchi OA and GRA to standardize the values of the responses for a better aeration performance.
- The arrangement of the experience N°.5 provided a high value of γ_i and the most potent multi-performance combination. By using the lowest power consumption capacity as the optimization target, the DD_L was the factor that revealed the highest sensitivity instead of the MLSS.
- The empirical model was built, and its outcomes showed that the predicted-R^2 was 0.9856 and the adjusted-R^2 was 0.9820. The MLR model had an R^2 > 80 %, confirming that the model is reliable.

Acknowledgments

The authors share their gratitude to Oran's Water and Sanitation Society (SEOR), the Algerian Ministry of Higher Education and Scientific Research (MESRS), the General Directorate for Scientific Research and Technological Development (DGRSDT), and the Natural Science Foundation of Shandong Province of China (ZR2020ME236) for their support. The authors would also like to thank Mr. TEFAHI Mehdi, the head engineer of (EL KERMA WWTPs of Oran city, Algeria) for supporting this scientific contribution.

References

[1] M. E. El Aissaoui El Meliani, A. Debab, M. Kheladi, A. Benhamou, (2019). Prediction et modelisation du coefficient (K_La) par respirometrie dans un bioreacteur a boues activees. *African review of science, technology and development, 4*, 39-45.

[2] D. Rosso, L. M. Jiang, R. Sobhani, B. Wett, (2012). Energy Footprint Modelling: a tool for process optimization in Large Wastewater Treatment Plants. *Water practice and technology, 7* (1).

[3] G. A. Baquero-Rodríguez, J. A. Lara-Borrero, D. Nolasco, D. Rosso, (2018). A Critical review of the factors affecting modeling oxygen transfer by fine-pore diffusers in activated sludge. *Water environment research*, *90*(5), 431-441.

[4] Wang, M., Mo, H., Liu, G. H., Qi, L., Yu, Y., Fan, H., Wang, H. (2020). Impact of scaling on aeration performance of fine-pore membrane diffusers based on a pilot-scale study. *Scientific reports*, *10*(1), 1-10.

[5] R. Oulebsir, A. Lefkir, A. Safri, A. Bermad, (2020). Optimisation of the energy consumption in activated sludge process using deep learning selective modeling. *Biomass bioenergy, 132,* 105-420.

[6] Füreder, K., Svardal, K., Frey, W., Kroiss, H., Krampe, J. (2018). Energy consumption of agitators in activated sludge tanks–actual state and optimization potential. *Water science and technology*, *77*(3), 800-808.

[7] Dao, N. T. M., Liu, B., Terashima, M., Yasui, H. (2019). Computational fluid dynamics study on attainable flow rate in a lamella settler by increasing inclined plates. *Journal of water and environment technology*, *17*(2), 76-88.

[8] Dao, N. T. M., Terashima, M., Yasui, H. (2019). Improvement of suspended solids removal efficiency in sedimentation tanks by increasing settling area using computational fluid dynamics. *Journal of water and environment technology*, *17*(6), 420-431.

[9] Gillot, S., Capela-Marsal, S., Roustan, M., Héduit, A. (2005). Predicting oxygen transfer of fine bubble diffused aeration systems—model issued from dimensional analysis. *Water research*, *39*(7), 1379-1387.

[10] M. R. Wagner, H. J. Pöpel, (1998). Oxygen transfer and aeration efficiency—influence of diffuser submergence, diffuser density, and blower type. *Water science and technology, 38,* 1-6.

[11] S. Bun, K. Wongwailikhit, N. Chawaloesphonsiya, J. Lohwacharin, P. Ham, P. Painmanakul, (2020). Development of modified airlift reactor (MALR) for improving oxygen transfer: optimize design and operation condition using design of experiment methodology. *Environmental. technology, 41*(20), 2670-2682.

[12] J. Behnisch, M. Schwarz, M. Wagner, (2020). Three decades of oxygen transfer tests in clean water in a pilot-scale test tank with fine-bubble diffusers and the resulting conclusions for WWTPs operation. *Water practice and technology, 15*(4), 910-920.

[13] M. Garrido-Baserba, R. Sobhani, P. Asvapathanagul, G. W. McCarthy, B. H. Olson, V. Odize, A. Al-Omari, S. Murthy, A. Nifong, J. Godwin, C. Bott, M. Stenstrom, A. Shaw, D. Rosso, (2017). Modelling the link amongst fine-pore diffuser fouling, oxygen transfer efficiency, and aeration energy intensity. *Water research, 111*, 127-139.

[14] R. Gori, A. Balducci, C. Caretti, C. Lubello, (2014). Monitoring the oxygen transfer efficiency of full-scale aeration systems: investigation method and experimental results. *Water science and technology, 70*(1), 8-14.

[15] D. H. Nguyen, (2014). Optimisation of the design and operation of wastewater treatment plants, Doctoral dissertation, University of Lorraine.

[16] G. Zhao, M. Garrido-Baserba, S. Reifsnyder, J. C. Xu, D. Rosso, (2019). Comparative energy and carbon footprint analysis of biosolids management strategies in water resource recovery facilities. *Science of the total environment*, *665*, 762-773.

[17] K. I. Ashley, K. J. Hall, D. S. Mavinic, (1991). Factors influencing oxygen transfer in fine pore diffused aeration. *Water research, 25*, 1479-1486.

[18] D. Rosso, S. E. Lothman, M. K. Jeung, P. Pitt, W. J. Gellner, A. L. Stone, D. Howard, (2011). Oxygen transfer and uptake, nutrient removal, and energy footprint of parallel full-scale IFAS and activated sludge processes. *Water research, 45*(18), 5987-5996.

[19] M. Terashima, M. So, R. Goel, H. Yasui, (2016). Determination of diffuser bubble size in computational fluid dynamics models to predict oxygen transfer in spiral roll aeration tanks. *Journal of water process engineering, 12*, 120-126.

[20] M. E. El Aissaoui El Meliani, A. Debab, A. Benhamou, T. Amen, M. Terashima, H. Yasui, (2020). Modelling the (α)-factor in a Pneumatic Bioreactor Using the Taguchi Approach. *International review* on *modeling* and simulations, *13*, 252-259.

[21] L. Nazari, Z. Yuan, M. B. Ray, C. C. Xu, (2017). Co-conversion of waste activated sludge and sawdust through hydrothermal liquefaction: optimization of reaction parameters using response surface methodology. *Applied energy*, *203*, 1-10.

[22] J. Rodier, C. Bazin, J. P. Broutin, P. Chambon, H. Champsaur, L. Rodi, (2009) Water Analysis, 9th Ed. Dunod, Paris, France, 15-79.

[23] E. Pittoors, Y. Guo, S. W. Van Hulle, (2014). Oxygen transfer model development based on activated sludge and clean water in diffused aerated cylindrical tanks. *Chemica. engineering journal, 243*, 51-59.

[24] K. Campbell, J. Wang, G. T. Daigger, (2020). Filamentous organisms degrade oxygen transfer efficiency by increasing mixed liquor apparent viscosity: Mechanistic understanding and experimental verification. *Water research, 173*, 115-570.

[25] Y. Amerlinck, G. Bellandi, A. Amaral, S. Weijers, I. Nopens, (2016). Detailed off-gas measurements for improved modeling of the aeration performance at the WWTPs of Eindhoven. *Water science and. technology, 74*, 203-211.

[26] M. Von Sperling, (2007). Basic principles of wastewater treatment, Volume 2. IWA publishing. London, UK,151.

[27] N. H. Naqiuddin, L. H. Saw, M. C. Yew, F. Yusof, H. M. Poon, Z. Cai, H. San Thiam, (2018) Numerical investigation for optimizing segmented micro-channel heat sink by Taguchi-Grey method. *Applied energy, 222*, 437-450.

[28] M. Sarıkaya, A. Güllü, A., (2014). Taguchi design and response surface methodology-

based analysis of machining parameters in CNC turning under MQL. *Journal of cleaner production*, *65*, 604-616.

[29] B. Liu, Y. Li, J. Wu, Y. Shao, F. Chen, J. H. Wu, R. Goel, M. Terashima, H. Yasui, (2020). Evaluating nitrite-oxidizing organism survival under different nitrite concentrations. *Water science and technology*, *82*(2), 273-280.

[30] A. A. Almetwally, (2020). Multi-objective Optimisation of woven fabric parameters using Taguchi–Grey relational analysis. *Journal of natural fibers*, *17*(10), 1468-1478.

[31] T. K. Bharadwaj, K. N. Gupta, (2021). Dye separation using a semi-batch foaming process: Process optimization using Taguchi methodology and Grey relational analysis. *Environmental engineering research*, *26*(4), 20-31.

[32] P. Painmanakul, J. Wachirasak, M. Jamnongwong, G. Hébrard, (2009). Theoretical prediction of volumetric mass transfer coefficient (K_La) for designing an aeration tank *Engineering journal, 13(3)*, 13-28.

[33] G. Sodeifian, S. A. Sajadian, N. Ardestani, (2017). Experimental optimization and mathematical modeling of the supercritical fluid extraction of essential oil from Eryngium billardieri: application of simulated annealing (SA) algorithm. *The journal of supercritical fluids*, *127*, 146-157.

[34] S. Gillot, F. Kies, C. Amiel, M. Roustan, A. Héduit, (2005). Application of the off-gas method to the measurement of oxygen transfer in biofilters. *Chemical engineering science*, *60*(22), 6336-6345.

[35] H. Fan, L. Qi, G. Liu, Y. Zhang, Q. Fan, H. Wang, (2017). Aeration optimization through operation at low dissolved oxygen concentrations: Evaluation of oxygen mass transfer dynamics in different activated sludge systems. *Journal of environmental sciences*, *55*, 224-235.

[36] Trambouze, P., Euzen, J. P. (2004). *Chemical reactors: from design to operation*. Technip Editions.

[37] K. K. Al-Ahmady, (2011). Mathematical model for calculating oxygen mass transfer coefficient in diffused air systems. *Al-Rafidain engineering journal (AREJ)*, *19*(4), 43-54.

[38] K. Wongwailikhit, P. Warunyuwong, N. Chawaloesphonsiya, N. Dietrich, G. Hébrard, P. Painmanakul, (2018). Gas sparger orifice sizes and solid particle characteristics in a bubble column–relative effect on hydrodynamics and mass transfer. *Chemical engineering and technology*, *41*(3), 461-468.

[39] J. Lee, (2020) Oxygen transfer rate and oxygen uptake rate in subsurface bubble aeration systems. *Journal of environmental engineering*, *146*(1), 0251-9003.

[40] L. Uby, (2019) Next steps in clean water oxygen transfer testing–A critical review of current standards. *Water research, 157*, 415-434.

[41] G. Skouteris, G. Rodriguez-Garcia, S. F. Reinecke, U. Hampel, (2020). The use of pure oxygen for aeration in aerobic wastewater treatment: a review of its potential and limitations. *Bioresource technology, 3*, 12, 123-595.

[42] H. Benmoussa, W. Elfalleh, S. He, M. Romdhane, A. Benhamou, R. Chawech, (2018) Microwave hydro-diffusion and gravity for rapid extraction of essential oil from Tunisian cumin (Cuminum cyminum L.) seeds: Optimisation by response surface methodology. *Industrial crops and products*, *124*, 633-642.

[43] Mueller, J., Boyle, W. C., Popel, H. J. (2002). *Aeration: Principles and practice, Volume 11*. CRC press.